# OPTIMAL DISTURBANCES OF FLOW ABOVE A FLAT PLATE WITH AN ELLIPTIC LEADING EDGE

**Antonios Monokrousos**[1]*, **Luca Brandt**[1], **Catherine Mavriplis**[2], **Dan S. Henningson**[1]
[1]Linné Flow Centre, SeRC, KTH Mechanics, SE-100 44, Stockholm, Sweden
[2]Department of Mechanical Engineering, University of Ottawa, ON, Canada, K1N 6N5

## ABSTRACT

Adjoint-based iterative methods are employed in order to compute linear optimal disturbances in the case of a spatially growing boundary layer around an elliptic leading edge. The Lagrangian approach is used where an objective function is chosen and constraints are assigned. The optimization problem is solved using power iterations combined with a matrix-free formulation, where the state is marched forward in time with a standard DNS solver and backward with the adjoint solver until a chosen criterion is fulfilled. We consider the global and the upstream localized optimal initial condition leading to the largest possible energy amplification at time $T$. We find that the two-dimensional initial condition with the largest potential for growth is a Tollmien-Schichting-like wave packet that includes the Orr mechanism and is located inside the boundary layer, downstream of the leading edge. The localized optimal initial condition method allows a more precise systematic study of leading edge effects; we propose it a new method to study receptivity. We find the two-dimensional disturbances are inefficient at triggering an unstable eigenmode. The three-dimensional disturbances exploit the lift up mechanism; both the global and upstream localized disturbances give significant growth. These findings support the hypothesis of high receptivity to three-dimensional disturbances.

## INTRODUCTION

The flat plate boundary layer has been a test-bed for various approaches when studying hydrodynamic stability. Its relevance arises from the fact that, even if is a fairly simple flow, it contains features of many external flows; thus it is a good model for them. In stability studies further simplified versions of the general case are often used with approximations like the locally-parallel assumption (Fourier decomposition in the streamwise direction (Butler & Farrell, 1992; Reddy & Henningson, 1993) or the slowly varying (parabolized equations (Andersson *et al.*, 1999; Luchini, 2000; Levin & Henningson, 2003; Tempelmann *et al.*, 2010)). Two and three-dimensional disturbances have been studied using global modes and offer an accurate representation of the stability of the growing boundary layer (Åkervik *et al.*, 2008). However the effect of the leading edge has not been considered so far.

Recently, with the development of the time-stepper technique (Tuckerman & Barkley, 2000), it has become possible to tackle more complicated flow cases with two and three-dimensional disturbances. Essentially stability studies are possible for any type of flow case and/or geometry for which a direct numerical simulation is feasible. The only requirement is a numerical solver of the time-dependent linearized Navier-Stokes equations and the corresponding adjoint problem. This approach was first adopted by Tuckerman & Barkley (2000) and later by Barkley *et al.* (2008) and Blackburn *et al.* (2008).

In Monokrousos *et al.* (2010) optimal disturbances for a case of a flat-plate boundary layer excluding the leading edge was studied. It was found that the optimal initial condition for short spanwise wavelengths are finite-length streamwise vortices exploiting the lift-up mechanism to create streaks. For long spanwise wavelengths it is the Orr mechanism combined with the amplification of oblique wave packets that is responsible for the disturbance growth. It is found that the latter mechanism is dominant for the long computational domain and thus for the relatively high Reynolds number considered here.

This project is an extension to previous work by Monokrousos *et al.* (2010) where optimal disturbances were computed for the case of the flat plate boundary layer. Here we take a step further and include the leading edge of the plate while retaining a fairly high Reynolds number where typically transitional or even turbulent flow is observed. In particular we focus on the effect of the leading edge, how it can change the optimal disturbances and how the boundary layer can be optimally excited by disturbances coming from the outside.

The flow case, for the chosen parameters is classified as noise amplifier, in contrast to an oscillator where more often standard modal analysis is performed. It is characterized by convectively instabilities when studied with the local approach. From the global point of view the flow is asymptotically stable to linear disturbances. Hence it is more relevant to look at the transient growth problem or non-modal analysis.

## FORMULATION

The equations to be solved are the linearized Navier-Stokes in the incompressible regime:

$$\partial_t \mathbf{u} + (\mathbf{U}\cdot\nabla)\,\mathbf{u} + (\mathbf{u}\cdot\nabla)\,\mathbf{U} = -\nabla p + Re^{-1}\Delta\mathbf{u}, \qquad (1)$$
$$\nabla\cdot\mathbf{u} = 0.$$

*antonios@mech.kth.se

where $\mathbf{U}$ is the base flow, $\mathbf{u}$ is a perturbation velocity, $p$ is pressure and *Re* is the Reynolds number.

The Lagrangian approach is used where an objective function is chosen and constraints are assigned. We are looking for stationary points of the Lagrange functional with respect to the different design variables where optimality is fulfilled. The method is equivalent to finding the leading eigenvalues of combined direct and adjoint Navier-Stokes evolution operator. The quantity we choose to maximize, *i.e.* the objective function, is the disturbance kinetic energy at the final time:

$$\mathscr{J}(\mathbf{u}) = (\mathbf{u}(T), \mathbf{u}(T)). \tag{2}$$

The chosen constraints are the demand for $\mathbf{u}$ to satisfy the linearized Navier-Stokes and, since we work in the linear framework, we force our initial condition to unit energy. Hence the Lagrangian functional is written as:

$$\mathscr{L}(\mathbf{u}, \mathbf{u}^*, \gamma) = \mathscr{J} - \int_0^T (\mathbf{u}^*, (\partial_t - \mathscr{A})\,\mathbf{u})\,\mathrm{d}t - \gamma((\mathbf{u}(0), \mathbf{u}(0)) - 1)\,. \tag{3}$$

where we rewrite the Navier-Stokes in the state space formulation

$$(\partial_t - \mathscr{A})\mathbf{u} = 0, \quad \mathbf{u}(0) = \mathbf{u}_0\,.$$

$\mathbf{u}^*$ and $\gamma$ are Lagrange multipliers. $\mathbf{u}^*$ is often called the adjoint variable. See Monokrousos *et al.* (2010) for more details.

To solve the optimization problem a matrix-free method is employed, where the state is marched forward in time with a standard direct numerical solver and backward with the corresponding adjoint solver until a chosen convergence criterion is fulfilled.

The problem is initialized with a random field, usually noise. The governing equations are iterated until the action of the combined forward and backward time marching corresponds to pure stretching of the initial condition, i.e. $p_0 = \lambda q_0$, with $q_0$ being the initial perturbation, $p_0$ the final field from the adjoint solution and $\lambda$ a scalar. At convergence $q_0$ is the optimal disturbance and also an eigenvector of the operator $\mathscr{H}^\dagger\mathscr{H}$ where $\mathscr{H}$ corresponds to the direct operator, also known as the propagator and $\mathscr{H}^\dagger$ to the adjoint: $\mathscr{H}^\dagger\mathscr{H}q_0 = \lambda q_0$. The action of $\mathscr{H}$ therefore amounts to integrating the linearized Navier-Stokes equations to final time $T$, where $T$ becomes a parameter of the optimization.

A similar procedure is applied to find the optimal initial condition localized upstream of the leading edge that undergoes the largest possible amplification as it travels downstream, penetrating the boundary layer. With this approach, we propose a systematic and direct method to compute the receptivity of the boundary layer to external disturbances as the computed optimal modes can be used as a projection basis to quantify the ability of incoming free-stream disturbances to initiate perturbations in the boundary layer. The formulation for localized optimal disturbances was first developed by Monokrousos *et al.* (2010). The optimization problem is slightly different from the one described above. The new Lagrangian reads

$$\begin{aligned}\mathscr{L}(\mathbf{u}, \mathbf{u}^*, \gamma) = (\mathbf{u}(T), \mathbf{u}(T)) - \int_0^T (\mathbf{u}^*, (\partial_t - \mathscr{A})\,\mathbf{u})\,\mathrm{d}t \\ -\gamma((\mathbf{u}(0), \mathbf{u}(0))_\Lambda - 1) - (\psi, \nabla\cdot\mathbf{u}(0))_\Lambda\end{aligned} \tag{4}$$

where the initial condition must exist only inside the subdomain $\Lambda$. Additionally the optimal perturbation must be divergence-free. The inner product defined by $(\cdot,\cdot)_\Lambda$ corresponds to an integral over $\Lambda$. Taking variations with respect to each variable gives:

$$\begin{aligned}\left(\frac{\partial\mathscr{L}}{\partial\mathbf{u}^*}, \delta\mathbf{u}^*\right) &\Rightarrow (\partial_t - \mathscr{A})\mathbf{u} = 0, \\ \left(\frac{\partial\mathscr{L}}{\partial\mathbf{u}}, \delta\mathbf{u}\right) &\Rightarrow (-\partial_t - \mathscr{A}^\dagger)\mathbf{u}^* = 0,\end{aligned} \tag{5}$$

along with two optimality conditions:

$$\begin{aligned}\mathbf{u}(0) &= \gamma^{-1}(\mathbf{u}^*(0) - \nabla\psi)|_\Lambda, \\ \mathbf{u}^*(T) &= \mathbf{u}(T)\,.\end{aligned}$$

For the full derivation we refer to Monokrousos *et al.* (2010).

## NUMERICAL APPROACH

The governing equations are solved within the spectral element code Nek5000, developed by Tufo & Fischer (2001). The linearized Navier-Stokes equations and the adjoint system are solved by a weighted residual spectral element method (Patera, 1984), which allows multi-domain decomposition while preserving high order accuracy. Inside each sub-domain, referred to as a spectral element, the pressure and velocity fields are represented by a tensor product of Legendre polynomial Lagrangian interpolants, N-2 and Nth order respectively. Gauss numerical quadrature is used to represent the integrals of the weak weighted residual formulation. Pressure is treated by Gauss and velocity by Gauss-Lobatto quadrature, entailing a staggered mesh and obviating the need for pressure boundary conditions. For further details see Fischer *et al.* (2008).

The modular operator and elemental approach of the Nek5000 code renders the implementation of the adjoint formulation straightforward: adjoint operators of Equation 5 are easily reformatted from existing operators of Equation 5a). Convective terms are advanced explicitly by a 3rd order Adams-Bashforth scheme in both the forward and backward problems. The self-adjoint diffusion terms are solved implicitly by a GMRES iterative solver, accelerated in the case of the pressure field with a projection technique (Fischer, 1998) that makes use of previous time step pressure modes for a high quality first guess. The optimization problem for the optimal initial condition is validated against previous results from Monokrousos *et al.* (2010).

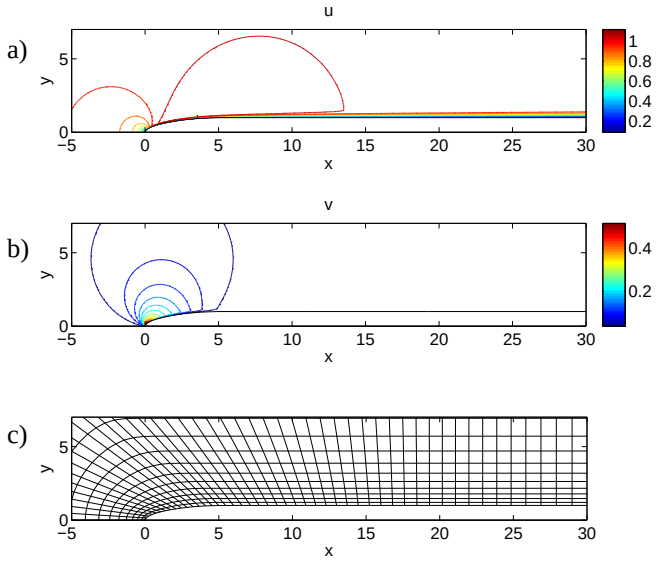


Figure 1. Contours of the streamwise (a) and wall-normal (b) velocity components of the base flow for $Re = 3000$. The plot has equal scaling in the two directions. c): The spectral element grid (without the Gauss-Lobatto Legendre points)

## Flow Case

We consider a flow around a flat plate with an elliptic leading edge. The leading edge is a modified super-ellipse:

$$\left(\frac{y}{b}\right)^2 = 1 - \left(\frac{a-x}{a}\right)^p \text{ where } p = 2 + \left(\frac{x}{a}\right)^2. \qquad (6)$$

that has zero curvature at the juncture with the flat section so that no disturbances are introduced by the plate itself. The ratio $\frac{a}{b}$ defines the bluntness and is chosen here $\frac{a}{b} = 6$ which corresponds to a relatively blunt shape, Schrader *et al.* (2010). The Reynolds number of the flow is $Re = \frac{bU}{\nu}$ based on the half thickness of the plate $(b)$, the free-stream velocity $(U)$ and the kinematic viscosity of the fluid $(\nu)$. The results presented correspond to Reynolds number $Re = 3000$.

In Figure 1a) and 1b) the two velocity components of the base flow are shown. Since the flow is globally stable, the base flow is computed by marching the full non-linear Navier-Stokes equations in time until a steady state is obtained. The boundary conditions imposed are those computed by solving the Euler equations in a domain much larger than our computational domain. A strong deceleration of the flow is observed near the stagnation point, as well as a strong vertical velocity component immediately downstream. Further downstream a thin boundary layer is developed. The computational box extends downstream $100-200$ units depending on the case. For a validation of the base flow see Schrader *et al.* (2010).

## Resolution

Using the spectral element method, we decompose the domain in several, relatively large elements. The present results are for polynomial order 9, which implies 100 points per element for the 2D case and 1000 for the 3D. The total number of elements depends on the length of the box. We run the 2D cases in a longer box (in order to be able to observe an unstable Tollmien-Schichting (TS) wave packet) using 3040 elements, 19 in the direction normal to the plate and 160 along the plate. The total number of points is 304000. In the 3D cases the computational box was shorter and thus we used 124 elements in the streamwise direction. However we needed 3 elements in the spanwise direction to resolve the modulation of the Fourier modes and this gives a total number of elements of 7068. Since these are 3D elements the total number of points is 7068000. In both cases we cluster the elements both in the wall-normal direction near the wall and along the plate near the area of the leading edge. A section of the computational grid located around the leading edge is shown in Figure 1c).

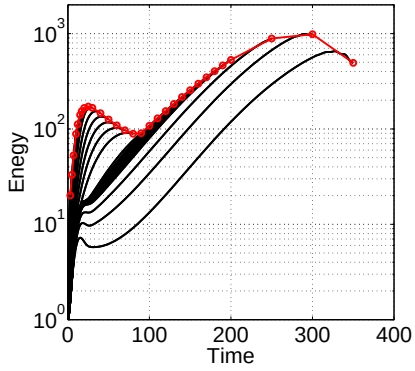


Figure 2. The black curves show disturbance energy vs optimization times for $Re = 3000$. The red curve is the energy envelope.

## RESULTS

We investigate the disturbances that give the largest transient energy growth. In order to determine the structure in question we loop over different optimization times. Additionally since the base flow is homogeneous in the spanwise direction, disturbances of different spanwise periodicity are considered separately. Owing to the cost of each optimization loop, relatively few cases are considered. However, we are confident that the optimal structures are captured and the essential physical mechanisms are included.

## Optimal Initial Conditions

We consider optimal initial conditions where no assumptions are made about the location. Two and three dimensional cases are studied.

### Two-Dimensional Disturbances

First we consider two-dimensional disturbances. Figure 2b) reports results for Reynolds number $Re = 3000$. In this case we observe that locally unstable TS-wave packets are generated and amplify exponentially as they are convected downstream. The maximum time for energy growth is governed here by the downstream extension of the computational box, indeed a longer box would yield longer optimization times and more space for

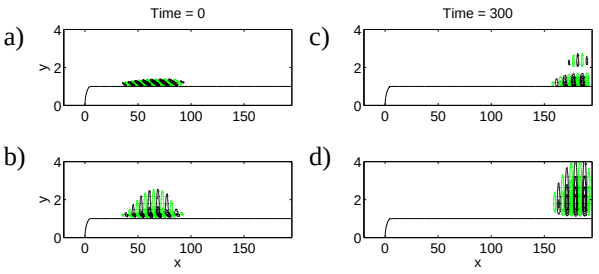


Figure 3. Spatial structures for two-dimensional optimal initial condition and the corresponding responses. $Re = 3000$: initial condition streamwise component a) and wall-normal component b). Response streamwise component c) and wall-normal component d).

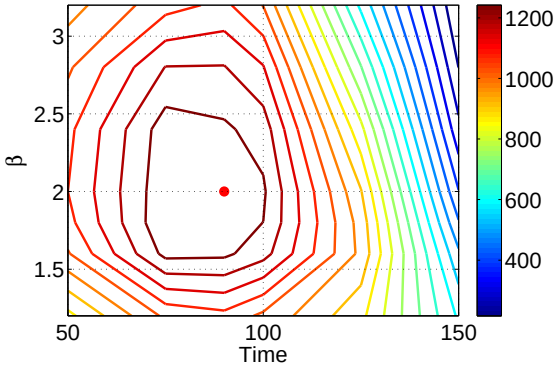


Figure 4. Contours of energy gain for different final times and spanwise wavenumbers. The red dot corresponds to the maximum energy gain. The levels are normalized with respect to the energy of the initial condition. The corresponding structures are shown in Figure 5

the exponential instability to grow. Additionally, we note a local maximum for short optimization times which corresponds again to a pure Orr-mechanism which is active on small time scales. The energy decay seen for large optimization time is due to the fact that these disturbances gradually exit our computational box; thus their measurable energy decays.

In Figure 3 the spatial structures of the optimal disturbances are shown where the optimal time is $T = 300$ ($Re = 3000$). The structures look rather similar, Orr-structures generating wave-packets, in both cases (also seen by Monokrousos *et al.* (2010) and Åkervik *et al.* (2008)).

**Three-Dimensional Disturbances** Considering three dimensional disturbances, one additional parameter enters the problem, namely the spanwise wavenumber $\beta$. To determine the optimal $\beta$ we need to loop over an additional parameter, as we do for the optimization time. These leads to a two-dimensional parameter space we need to explore.

In Figure 4 we plot iso-contours of energy gain for different optimization times $T$ and spanwise wavenumbers $\beta$. We see a clear peak at time, $T = 90$ and spanwise wavenumber $\beta = 2.0$. In an attempt to understand the physical mechanisms

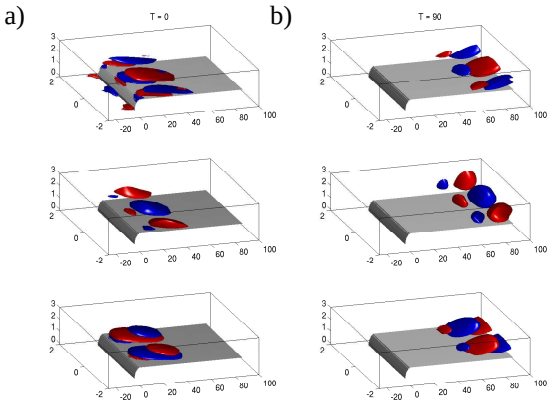


Figure 5. Isosurfaces of the disturbance velocity of the three-dimensional optimal initial condition $(a)$ and the corresponding flow response $(b)$. The three components shown are streamwise, wall-normal and spanwise (from top to bottom). The energy gain is $G = 1.3 \cdot 10^3$. The contour level of the is chosen 30% of the maximum. Red corresponds to positive and blue to negative disturbance velocity.

behind it we look at the spatial distribution of the disturbance velocities. The three components of the optimal initial condition are shown in Figure 5a) and the corresponding response in 5b) while the component-wise energy content is shown in Table 1.

In Table 1 we see a strong component-wise energy transfer which implies that the lift-up mechanism is active: streamwise vortices induce streamwise streaks inside the boundary layer. Similar results were obtained by Andersson *et al.* (1999) using the boundary layer equations and by Monokrousos *et al.* (2010) in the global framework without the leading edge. We observe that most of the initial energy is in the spanwise and wall-normal direction, implying the existence of streamwise vortices that generate a large response is the form of streamwise streaks which are seen in Figure 5b). Additionally we see that the Orr-mechanism with the characteristic upstream leaning structures contributes to some energy gain.

From Figure (4) we see a rapid decay of the amplification for long optimization times due to the limited box size. The disturbance is forced to move upstream, in order to avoid leaving the domain within that time and at some point it goes upstream from the plate, towards the area of the flow where there is no shear. On the other hand for short times, the lift-up mechanism does not have enough time to fully exploit the shear of the boundary layer.

As mentioned above the reported Reynolds number is calculated based on the free-stream velocity, the half-width of the plate and the fluid viscosity. This implies that all lengths and hence wavenumbers are scaled with the half-width of the plate. In order to compare with the results from previous studies like Monokrousos *et al.* (2010), where the wavenumber is scaled with the displacement thickness, the length is multiplied with the ratio of the two Reynolds numbers since the free-stream velocity and the viscosity are equal in both cases. In those units the optimal wavenumber is $\beta^* = 0.67$ which is comparable to the value retrieved by Monokrousos *et al.*

| | Initial disturbance | Response |
|---|---|---|
| Streamwise | 6.3 % | 91.3% |
| Wall-normal | 28.6% | 1.8 % |
| Spanwise | 65.1% | 6.9% |

Table 1. Energy content of each component for the three-dimensional optimal initial and final condition. The energy gain is $G = 1.3 \cdot 10^3$. We observe a large component-wise energy transfer.

(2010) ($\beta^* = 0.55$). A variation is to be expected due to the inclusion of the leading edge in the computation.

## Localized Optimal Initial Conditions

We study optimal initial conditions that are forced to be localized in space. The method used is extensively described in Monokrousos *et al.* (2010). These type of optimal initial conditions allow us to study how a disturbance optimally penetrates the boundary layer around the curved leading edge and subsequently generates a perturbation that can have a strong growth downstream inside the boundary layer.

**Two-Dimensional Disturbances** First we study two-dimensional disturbances. We enforce the perturbations to exist in a sub-domain upstream from the leading edge. The optimization procedure gives the optimal shape within that domain, allowing us to specifically study the receptivity features. The results we obtain for this case are much in line with those of Schrader *et al.* (2010). The upstream-localized disturbances prove to be rather inefficient in penetrating the boundary layer. They lose a lot of energy during that phase and furthermore, the generated disturbance inside the boundary layer consists of a wavepacket characterized by a relatively high streamwise wavenumber compared to the one corresponding to the most unstable. Consequently the exponential instability is not efficiently initiated resulting in weak growth in the process.

It appears that the optimization procedure favors a stable wave-packet over the unstable one since it probably has better penetration properties (for this bluntness), that is, it loses less energy during the penetration procedure and thus is more optimal than the unstable one. To enhance the unstable wavepacket we would need a much longer computational domain with sufficient space for it to grow exponentially, which would render this computation very expensive.

**Three-Dimensional Disturbances** As before we perform a parametric study to find the optimal time and spanwise wavenumber $\beta$. In Figure 6 iso-contours of energy gain for different optimization times and spanwise wavenumbers are shown for the case of the upstream localized disturbance. The red dot corresponds to the maximum. The optimal disturbance occurs for time $T = 125$ and spanwise wavenumber $\beta = 2.8$. Comparing the values to the non-localized optimal we see two main differences. First the optimization time

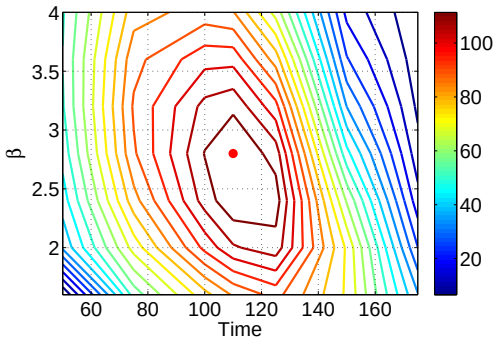


Figure 6. Contours of energy gain of localized optimal initial conditions for different final times and spanwise wavenumbers. The red dot corresponds to the maximum energy gain. The levels are normalized with respect to the energy of the initial condition. The levels are normalized with respect to the energy of the initial condition.

| | Initial disturbance | Response |
|---|---|---|
| Streamwise | 17.7 % | 93.6% |
| Wall-normal | 36.7% | 1.8 % |
| Spanwise | 45.6% | 4.6% |

Table 2. The table shows the component-wise energy content of each component for the initial and final condition. The energy gain was $G = 1.2 \cdot 10^2$

is longer and also $\beta$ is higher. The increased time was expected since the perturbation spends some time upstream from the leading edge and during the penetration phase. Additionally the total energy gain is lower but this is expected since we enforce to structure to be in a certain region and this leads to less than the global optimal performance.

We have seen already that the receptivity to purely two-dimensional disturbances is very weak and that can possibly explain why the optimal $\beta$ is increased for the upstream localized case, it may become less optimal with respect to the lift-up mechanism but at the same time it is less damped by the leading presence of the leading edge. The two trends seem to balance at $\beta = 2.8$ ($\beta^* = 0.93$).

The physical mechanisms pertaining to energy gain appear to be the same with the exception that the Orr-mechanism is not present. This is attributed to the fact that there is no shear where the perturbation is initiated hence no energy can be gained from an upstream leaning structure.

From Table 2 we see that most of the energy of the perturbation lies in the normal to the streamwise direction components and also the streamwise structure is almost constant implying streamwise vortices that generate streaks downstream inside the boundary layer.

The total energy gain is substantially weaker relative to the non-localized optimals. This can be attributed to the following: in this case the Orr-mechanisms can not contribute (no shear in the initial phase) and also the lift-up effect is

happening further upstream relative to the non-localized case which corresponds to lower Reynolds number and thus lower transient growth potential, see Andersson *et al.* (1999).

## CONCLUSIONS

We have applied a Lagrange multiplier technique using the direct and adjoint linearized Navier-Stokes equations in order to quantify the disturbance growth potential in a flow around a flat plate with an elliptic leading edge at moderately high Reynolds numbers. We consider the optimal initial condition leading to the largest possible energy amplification at time $T$. Additionally we compute the localized optimal disturbance upstream from the leading edge. This method can be used to create a modal basis and project free-stream disturbances *i.e.* a direct method for computing receptivity coefficients for externally excited flows. The optimization framework adopted does not restrict us to assume slow variation of the base flow in the streamwise direction, common to both the first order approximation of the Orr–Sommerfeld/Squire formulation and the more advanced Parabolized Stability Equations approximation; moreover, it allows us to include curved geometries and fully three dimensional configurations.

We find that the two-dimensional initial condition with the largest potential for growth is a TS-like wave packet that includes the Orr mechanism in their initial phase and is located inside the boundary layer, downstream of the leading edge. Its growth is linked to the exponentially unstable eigenmodes of the Blasius boundary layer and is limited by the streamwise extent of the computational box. The three dimensional case shows a peak in the energy much earlier in time (and space) for spanwise wavenumber $\beta = 2.0$, relevant to the well understood lift-up mechanism. This number is in close agreement with earlier studies of similar nature.

The localized optimal initial conditions are more interesting since they allow for better understanding of the effects of the leading edge and its receptivity properties. Disturbances are placed upstream in the free-stream. We find that the two-dimensional disturbances are rather inefficient at triggering an unstable wave-packet in order to exploit the convective instability of the boundary layer. The flow around the leading edge has a strong effect on these type of disturbances, *i.e.* it has a strong damping effect and the later evolution of the disturbance is dominated by this effect. In particular a stable wave-packet is generated and its energy just decays as it propagates downstream inside the boundary layer. This indicates that the unstable wave-packet is so strongly damped by the leading edge flow that is never favored by the optimization.

The three-dimensional disturbances though exploit the lift up mechanism very efficiently at a very early stage. The generated streaks are located further from the wall than the TS-wave and thus do not suffer from the loss of energy due to diffusion to the free-stream. Additionally, their streamwise wavenumber is very low and does not seem to be heavily affected by the low local Reynolds number in the area. This mechanism is proven to be very robust.

## ACKNOWLEDGEMENTS

The authors wish to thank Dr. Lars-Uve Schrader for providing the mesh generator and for many fruitful discussions. Computer time provided by SNIC (Swedish National Infrastructure for Computing) is gratefully acknowledged. The present work is supported by the Swedish research council which is gratefully acknowledged.

## REFERENCES

Åkervik, E., Ehrenstein, U., Gallaire, F. & Henningson, D. S. 2008 Global two-dimensional stability measures of the flat plate boundary-layer flow. *Eur. J. Mech. B/Fluids* **27**, 501–513.

Andersson, P., Berggren, M. & Henningson, D. S. 1999 Optimal disturbances and bypass transition in boundary layers. *Phys. Fluids* **11**, 134–150.

Barkley, D., Blackburn, H. M. & Sherwin, S. J. 2008 Direct optimal growth analysis for timesteppers. *Itn. J. Numer. Meth. Fluids* **57**, 1435–1458.

Blackburn, H. M., Barkley, D. & Sherwin, S. J. 2008 Convective instability and transient growth in flow over a backward-facing step. *J. Fluid Mech.* **608**, 271–304.

Butler, K. M. & Farrell, B. F. 1992 Three-dimensional optimal perturbations in viscous shear flow. *Phys. Fluids A* **4**, 1637–1650.

Fischer, P.F. 1998 Projection techniques for iterative solution of with successive right-hand sides. *Computer Methods in Applied Mechanics and Engineering* **163** (1-4), 193 – 204.

Fischer, P.F., Lottes, J.W. & Kerkemeier, S.G. 2008 nek5000 Web page. Http://nek5000.mcs.anl.gov.

Levin, O. & Henningson, D. S. 2003 Exponential vs algebraic growth and transition prediction in boundary layer flow. *Flow, Turbulence and Combustion* **70**, 183–210.

Luchini, P. 2000 Reynolds-number-independent instability of the boundary layer over a flat surface: Optimal perturbations. *J. Fluid Mech.* **404**, 289–309.

Monokrousos, A., Åkervik, E. & Henningson, L. Brandt D.S. 2010 Global three-dimentional optimal disturbances in the blasius boundary-layer flow using time-steppers. *J. Fluid Mech.* **650**, 181–214.

Patera, Anthony T 1984 A spectral element method for fluid dynamics: Laminar flow in a channel expansion. *Journal of Computational Physics* **54** (3), 468 – 488.

Reddy, S. C. & Henningson, D. S. 1993 Energy growth in viscous channel flows. *J. Fluid Mech.* **252**, 209–238.

Schrader, L.-U., Brandt, L., Mavriplis, C. & Henningson, D. S. 2010 Receptivity to free-stream vorticity of flow past a flat plate with elliptic leading edge. *Journal of Fluid Mechanics* **653** (-1), 245–271.

Tempelmann, D., Hanifi, A. & Henningson, D.S. 2010 Spatial optimal growth in three-dimensional boundary layers. *Journal of Fluid Mechanics* **646**, 5–37.

Tuckerman, L.S & Barkley, D. 2000 *Bifurcation Analysis For Timesteppers*, pp. 453–566. *Numerical Methods for Bifurcation Problems and Large-Scale Dynamical Systems* . Springer, New York.

Tufo, H.M. & Fischer, P.F 2001 Fast parallel direct solvers for coarse grid problems. *Par. & Dist. Computing* **61(2)**, 151–177.